IN-SITU DIAGNOSTICS ON FS-LASER INDUCED MODIFICATION OF GLASSES FOR SELECTIVE ETCHING

Martin Hermans*[a], Jens Gottmann[a], Anna Schiffer[b]
[a]Chair for Lasertechnology, RWTH Aachen University, Germany;
[b]Chair for Lasertechnology, RWTH Aachen University, Germany; now at: Department of Chemistry and 4D LABS, Simon Fraser University, Canada

*martin.hermans@llt.rwth-aachen.de; phone +492418906471; fax +492418906121; www.llt.rwth-aachen.de

ABSTRACT

In-situ observation of the in-volume modification of glasses by focused ultra-short pulsed laser radiation with an interferometer microscope allows for the spatially resolved measurement of the transient optical path difference (OPD) in the surrounding of the laser-induced modification. By the relation of refractive index and temperature an estimation of temperature during modification process is possible. The absorption of the laser radiation is measured and is, together with the estimation of processing temperature during modification, a first step towards a process model for the induced modifications of the transparent material.

Keywords: interferometry, in-volume modification, in-situ, absorption, ultra-short pulsed

1. INTRODUCTION

The manufacture of transparent micro components, microfluidic systems and integrated optical systems, such as waveguides, is an important development for future technologies. The irradiation of dielectrics with focused ultra-short pulsed laser radiation enables the in-volume modification of the material and thus processing of waveguides, microparts, microchannels and crackless markings. The modification induces a permanent refractive index change [1] and a change in the etchability of the material [2]. The modification is caused by the nonlinear absorption of fs-laser radiation [3]. Defects like color centers and oxygen vacancies are induced in the focal volume, contributing to the remanent modification in the material [4]. The heating, melting and re-solidification of the material causes a density redistribution and induces permanent stress [5], which also contributes to the refractive index change and to the corrodibility of the material. Heat accumulation effects occur for large repetition rates and small scanning velocities, inducing modification of volumes larger than the focal volume [6]. Heat accumulation and heat diffusion induce a transient heating and thus refractive index change in the vicinity of the focal volume, resulting in a laser-induced thermal lens and in aberrations. The resulting remanent modifications depend on the parameters scanning velocity, pulse energy, repetition rate and numerical aperture of the focusing lens. The aforementioned modification processes of glass are not fully understood. In order to develop an applicable process for industrial use, further investigation is needed. The processing temperature within the material is a central processing parameter corresponding to the resulting modification, which to the author's knowledge has not been investigated so far. The temperature as a processing parameter is important to understand the modification processes and the resulting vitreous phase. Furthermore, the correlation between the temperatures and the resulting modifications, resulting etchability and waveguiding properties can be investigated. Different theories and simulations can be tested by the measurement of the temperatures during material processing [7]. In-situ process diagnostic by interference microscopy and emission spectroscopy enables the investigation of a correlation between the observed experimental data and the resulting modifications. The emitted spectrum provides information on the origin of the emitted radiation: electronic relaxation or thermal radiation. Interference microscopy provides information on occuring refractive index changes by heat accumulation and thermal lensing.

2. EXPERIMENTAL SETUP & METHODS OF ANALYSIS

2.1 Interference Microscopy

A Mach-Zehnder interferometer combined with a microscope enables spatially resolved information on the optical path difference (OPD). The integrated microscope consists of a condenser for specimen illumination and an imaging objective. The in-volume modification with fs-laser radiation is enabled by using the imaging objective of the interference microscope as a focusing objective. Thus, a coaxial in-situ analysis of the refractive index change is possible.
The interference microscope is operated with a CCD camera and enables the time averaging observation of the transient refractive index change with a temporal resolution of 3 ms.
The illumination of the Mach-Zehnder interference microscope (Figure 1) is provided by a 660 nm LED. The specimen of interest is illuminated with Köhler illumination, realized by a system of lenses and apertures. The illuminating light beam is divided into two partial beams by a beam splitter. The partial beams are coherent to one another. Both beam paths are equipped with identical condensers, objectives, laser mirrors and specimens, providing identical optical paths. One beam passes through the object of interest treated with laser radiation while the other acts as a reference. An interference pattern is merely observed for an OPD smaller than the temporal coherence length of the illuminating light source. Therefore all optical components need to be of equivalent optical quality due to a small resulting OPD between both interferometer arms. Especially the integrated condensers and objectives have to match in terms of phase alteration. The degree of phase alteration match determines the resulting contrast of the interference pattern. A precise adjustment of the included optical components is required to achieve a high contrast interference pattern.

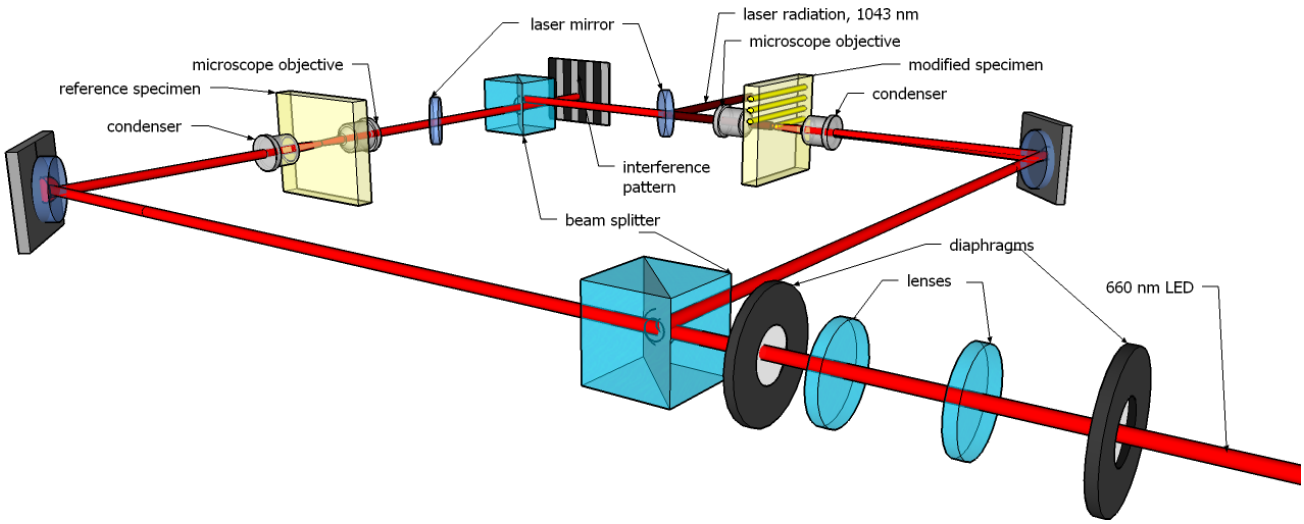

Figure 1. Schematic illustration of the experimental setup for the Mach-Zehnder interferometer

The laser beam is coupled into the interferometer by a coated mirror and propagates collinearly regarding the illuminating beam. A vertically aligned interference pattern is required for further analysis using a MATLAB program. The OPD within the observation path leads to a modified interference pattern with displaced interference fringes (Figure 2 right). A displacement to the right indicates a positive OPD and thus a positive refractive index change within the modified specimen. The MATLAB program provides an automated analysis of images from interference microscopy. The analysis proceeds row by row after calculating a reference interference pattern for each interference image. An example for a modified interference image (Figure 2) is the interference pattern resulting from an induced OPD in Borofloat 33. The material is processed at 1000 kHz repetition rate, an applied pulse energy of 400 nJ and a scanning velocity of 1.00 mm/s.
In order to calculate the OPD from fringe displacement, a reference interference pattern must be available. Reference images are not available for images from in-situ interference microscopy because the specimen has a wedge shape. While processing the material, the observation area is moving to different thicknesses of the specimen material and thus

an OPD change occurs, resulting into a constant drift of the interference fringe positions. Unmodified areas in each interference image are therefore used to calculate the reference interference pattern from fitting a *sin²* function to the pixel intensity distribution. The sin² fit is used for the determination of the wavelength and the phase shift from top to bottom of the analysed interference image. In order to calculate the OPD, the extrema values of the reference interference image and modified interference image must be equal. For each pixel row the elimination of noise and the extrapolation to equal extrema values enables the mapping of reference fringes to experimental data. Intensity

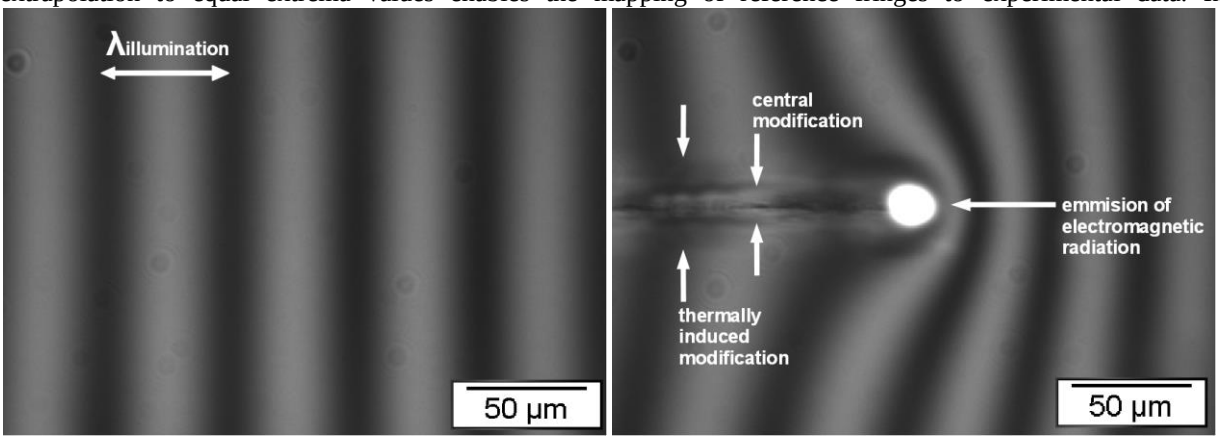

Figure 2 Undisturbed interference pattern with a 660 nm LED as illumination source (left). Interference pattern during in-volume modification of borosilicate glass (right). (parameter settings: 1000 kHz; 1:00 mm/s, 395 nJ)

fluctuations within a pixel row are caused by noise and remanent modifications. Identical extrema values from the reference interference image and the modified interference image are generated by a linear extrapolation of intensity. Each pixel of the modified interference pattern is assigned to a corresponding pixel position in the reference interference pattern. The magnitude of the optical path difference corresponds to the distance between the two assigned positions, measured in px. The measured optical path difference in px corresponds to an optical path difference in nm, depending on the central wavelength of the illumination light source. The OPD sign is determined by the direction of fringe displacement, according to the phase calibration of the interference microscope. The OPD is calculated for each pixel and depicted in a color plot.

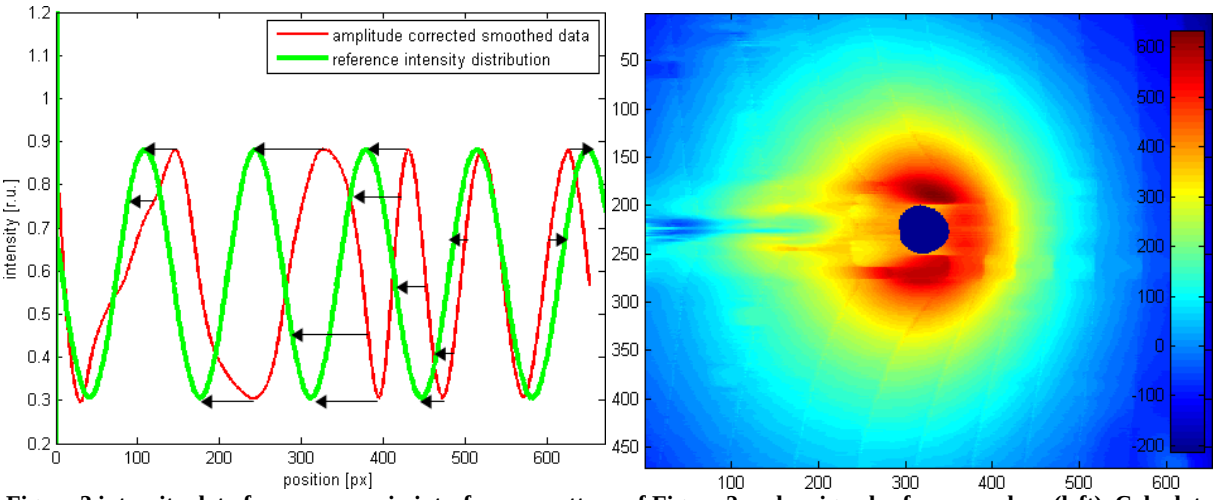

Figure 3 intensity data from one row in interference pattern of Figure 2 and assigned reference values (left). Calculated phase image of image (right) with OPD in nm.

The OPD of each pixel provides information on the sum of refractive index change in coaxial direction. The calculation of the spatial refractive index distribution is possible by performing tomography. Tomography requires information on the OPD in lateral direction, which is matter of on-going research.

The maximum OPD value corresponds to a positive maximum refractive index change and thus a larger temperature [8,9].

2.2 Absorbed Pulse Energy

According to Miyamoto et al [7], the absorptivity of glass depends on the repetition rate and the applied pulse energy in particular. The absorbed pulse energy is investigated using a micro positioning system and a power meter (Figure 4).

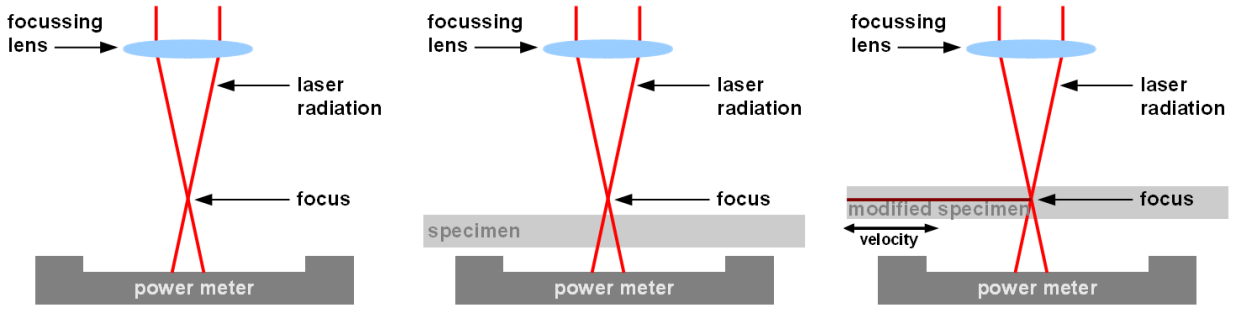

Figure 4 Measurement of applied average laser power at repetition rate (left), reference measurement of transmitted average power P_{ref} with defocused laser beam (middle), measurement of transmitted average power P_{trans} with focused laser beam and moving specimen.

The applied pulse energy E_{app} is calculated by the measured applied average power P_{app} at a repetition rate f_{rep}:

$$E_{app} = \frac{P_{app}}{f_{rep}}$$

A reference measurement of average power P_{ref} is performed with the laser radiation propagating through the specimen to take reflections into account, scattered radiation is neglected. The measurement of transmitted average power P_{trans} is conducted by focusing the laser radiation within the volume of the specimen and moving the specimen at constant velocity. The difference in transmitted power is equal to the absorbed power $P_{abs} = \Delta P = P_{ref} - P_{trans}$ and corresponds to the amount of absorbed pulse energy. The absorptivity A is calculated by the measured quantities P_{ref} and P_{trans}:

$$A = \frac{P_{abs}}{P_{trans}} = \frac{P_{ref} - P_{trans}}{P_{ref}}$$

The resulting absorbed pulse energy E_{abs} is determined by the measured quantities P_{ref} , P_{trans} and P_{app}:

$$E_{abs} = A \cdot E_{app} = \frac{P_{ref} - P_{trans}}{P_{ref}} \cdot \frac{P_{app}}{f_{rep}}$$

The absorptivity is investigated for various parameter settings and the results are analyzed in dependence of the material, the repetition rate and scanning velocity.

2.3 Light Microscopy

The remanent modifications and their morphology are investigated by optical bright field microscopy in top view and cross section. The width and height of the modifications are measured, considering the differentiation between the central modification and the heat affected zone HAZ (Figure 5).

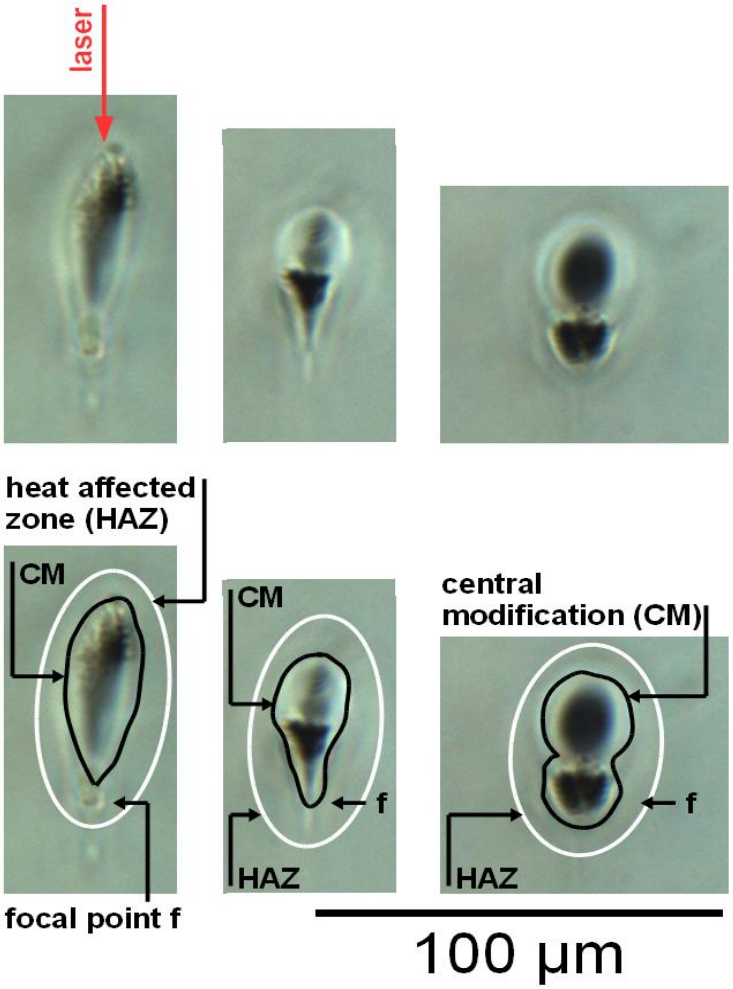

Figure 5 Cross sections of modifications in Borofloat 33, showing central modifications and heat affected zones (HAZ)

3. RESULTS & DISCUSSION

3.1 Absorptivity

The absorptivity A in Borofloat 33 was investigated for different parameter settings, whereas the maximum provided average laser power is limited to P_{app} < 900mW. The absorptivity for f_{rep} = 500 kHz can be investigated up to an applied pulse energy of E_{app} < 800 nJ. The absorptivity for f_{rep} = 1000 kHz is investigated for applied pulse energies E_{app} < 400 nJ. The absorptivity A for v = 0.25 mm/s increases with larger applied pulse energy E_{app} from A = 5% to A > 50% (Figure 6). The absorptivity A increases with a larger repetition rate, increasing from A = 34% to A = 46% at equal applied pulse energy E_{app} = 700 nJ. For f_{rep} = 1000 kHz and v = 0.25mm/s the absorptivity A is smaller than 23%.
For v = 1.00 mm/s the absorptivity A increases with larger applied pulse energy from A = 5% to A = 70% (Figure 6 right). The absorptivity A increases with the repetition rate f_{rep} for E_{app} > 100 nJ, especially from A = 25% to A = 61% at equal applied pulse energy E_{app} = 400 nJ. The absorptivity A is equal for f_{rep} = 500 kHz and f_{rep} = 1000 kHz for applied pulse energies E_{app} < 300 nJ within the limits of measuring accuracy of 5%.
The absorptivity A increases with increasing scanning velocity v for f_{rep} = 1000 kHz, increasing from A(0.25 mm/s) = 23% to A(1.00 m/s) = 61% at equal applied pulse energy E_{app} = 400 nJ. For f_{rep} = 500 kHz the absorptivity increases with larger scanning velocity v from A = 44% to A = 63% at equal applied pulse energy E_{app} = 600 nJ (Figure 6). The

absorptivity for f_{rep} = 100 kHz is independent on the scanning velocity v for all applied pulse energies E_{app} within the limits of measuring accuracy. The maximum absorptivity A = 70% is observed for v = 1.00 mm/s and f_{rep} = 500 kHz.
A larger absorptivity A is observed for increasing repetition rate f_{rep} and scanning velocity v for applied pulse energies E_{app} > 400 nJ.

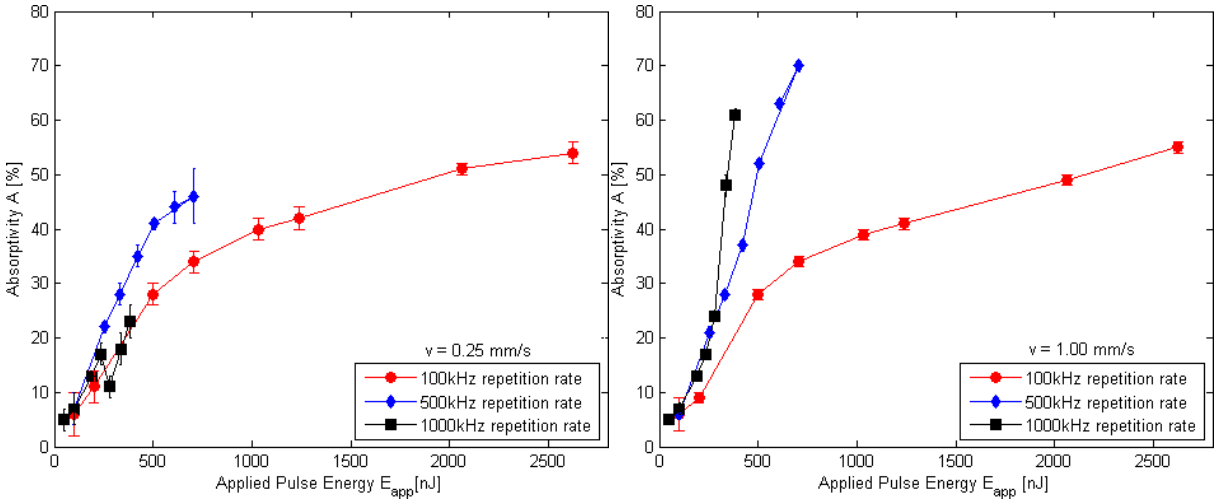

Figure 6 Absorptivity *A* in Borofloat 33 for *v* = 0.25 mm/s (left) and *v*=1.00 mm/s for three repetition rates.

A larger repetition rate f_{rep} leads to a larger temperature T within the material due to heat accumulation effects. The absorption volume increases with the number of pulses absorbed in one spot. The number of pulses per spot is reduced by a larger scanning velocity v and thus an absorption in a smaller absorption volume is caused. A larger scanning velocity v thus causes the absorption of laser pulses in a smaller absorption volume. The deposition of pulse energy in a smaller absorption volume leads to a larger temperature T. An increasing number of electrons is thermally excited into the conduction band with increasing temperature T. larger number of thermally excited electrons enables a larger absorption by avalanche ionization. Thus, a larger repetition rate enables a larger absorptivity in the material. The increasing absorptivity for v = 1.00 mm/s with increasing repetition rate f_{rep} for E_{app} > 100 nJ illustrates the need of further investigation of f_{rep} > 100 kHz with larger applied pulse energies, as well as the investigation at larger scanning velocities. The efficient absorption for high repetition rates and large velocities could enable the fast, precise and energy efficient modification of glass.

3.2 Interference Microscopy

The optical path difference (OPD) is calculated for each image pixel by the MATLAB program, resulting in a phase image for each interference image. The phase images are analyzed in dependence on the absorbed pulse energy E_{abs} and absorbed energy along travelpath E_{tp}. In order to compare the different parameter settings and find a general physical quantity, the modifications are investigated for equal absorbed energy E_{abs} along a path in the material. The physical quantity absorbed pulse energy along travelpath E_{tp} depends on v, f_{rep} and E_{abs} and is defined as:

$$E_{tp} = \frac{E_{abs} \cdot f_{rep}}{v}$$

The transient OPD is observable above a certain absorbed pulse energy threshold. The transient OPD is caused by heat accumulation and the larger refractive index of the material with a larger temperature [8, 9]. The maximum OPD in Borofloat 33 increases with the absorbed pulse energy E_{abs} up to OPD > 600nm (Figure 7). With increasing repetition rate f_{rep} the maximum OPD increases for equal absorbed pulse energy E_{abs}. For equal repetition rates f_{rep} the maximum OPD for both investigated scanning velocities are equal within the limits of measuring accuracy.

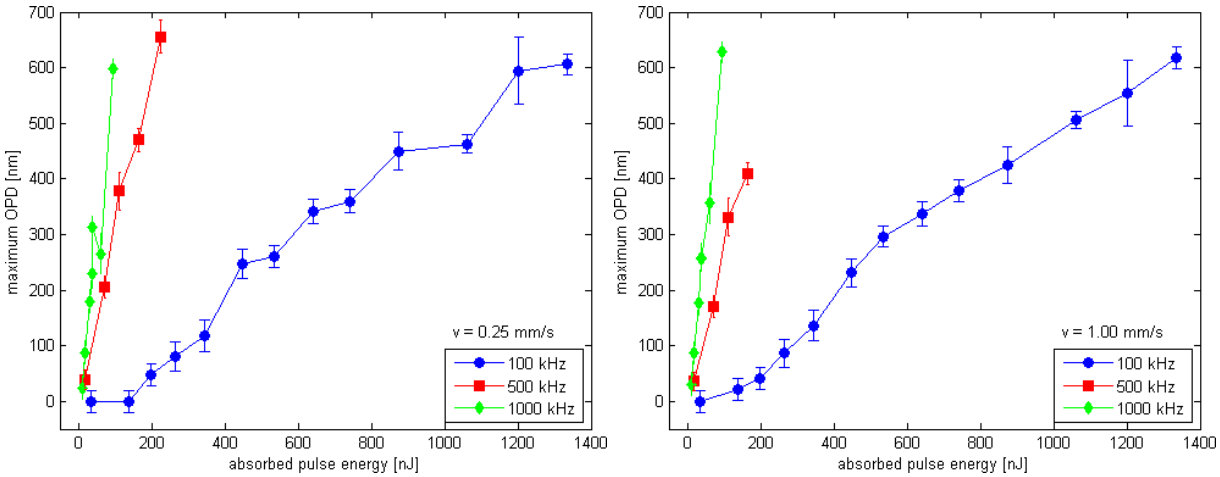

Figure 7 Maximum OPD in Borofloat 33 for v = 0.25mm/s (left) and 1.00 mm/s (right) for the investigated repetition rates f_{rep}.

The maximum OPD value increases with larger absorbed pulse energies E_{abs} from OPD < 50nm to OPD > 500nm (Figure 7). For absorbed pulse energies E_{abs} > 100 nJ the emission of radiation is observable around the focal point and overexposes the CCD chip, thus eliminating the information on the OPD in that area. The resulting OPD depends on the transient refractive index change within the material, caused by the heating of the material around the focal volume and heat accumulation and the height of the structure. An increasing temperature causes a larger refractive index of the material [8, 9].

In order to give an estimation of the mean temperature around the central modification the induced refractive index change Δn has to be calculated, depending on the assumed OPD causing thickness d. The calculated Δn corresponds to a temperature change ΔT. The coefficient dn/dT for Borofloat 33 is assumed to be equal to the to the thermal expansion coefficient α, which is $\alpha = 3.0 \cdot 10^{-6}\, 1/K$ in Borofloat 33 [10].The coefficient dn/dT is a 2.5-fold larger for temperatures $T > T_G$, with T_G as the transformation temperature T_G = 525 °C in Borofloat 33 [10] due to translational degrees of freedom which become available by liquidation. The refractive index change Δn(525 °C)= $= 1.5 \cdot 10^{-3}$ corresponds to the transformation temperature T_G = 525 °C. The temperature change ΔT is calculated for a refractive index change Δn by:

$$\Delta T = \frac{\Delta n}{3.0 \cdot \frac{10^{-6}}{K}} (T < T_G = 525°C)$$

$$\Delta T = \frac{\Delta n}{7.5 \cdot \frac{10^{-6}}{K}} + 300°C (T > T_G = 525°C)$$

Assuming the central modification as the heat source within the material, a maximum refractive index change Δn_{max} is calculated to estimate the maximum temperature T_{max} within the material. The maximum refractive index change is calculated by the maximum OPD divided by the height of the central modification h_{mod}.

A constant refractive index change $\Delta n_{max} \sim 22 \cdot 10^{-3}$ is observed in Borofloat 33 for v = 0.25 mm/s, f_{rep} = 100 kHz and E_{abs} > 1000 nJ. For the other parameters, Δn_{max} increases with larger absorbed pulse energies E_{abs}. The maximum Δn_{max} is observed for f_{rep} = 1000 kHz and both scanning velocities with $\Delta n_{max} \sim 40 \cdot 10^{-3}$, which corresponds to a temperature change of $\Delta T_{max} \sim 5300$ K. The maximum refractive index change for f_{rep} = 100 kHz is constant for absorbed pulse energies E_{abs} > 900 nJ within the limits of measuring accuracy, and corresponds to a temperature change of $\Delta T_{max} \sim 3000\ K$. The temperature change is calculated by the assumed coefficient dn/dT and plotted against the absorbed energy along travelpath E_{tp} (Figure 9).

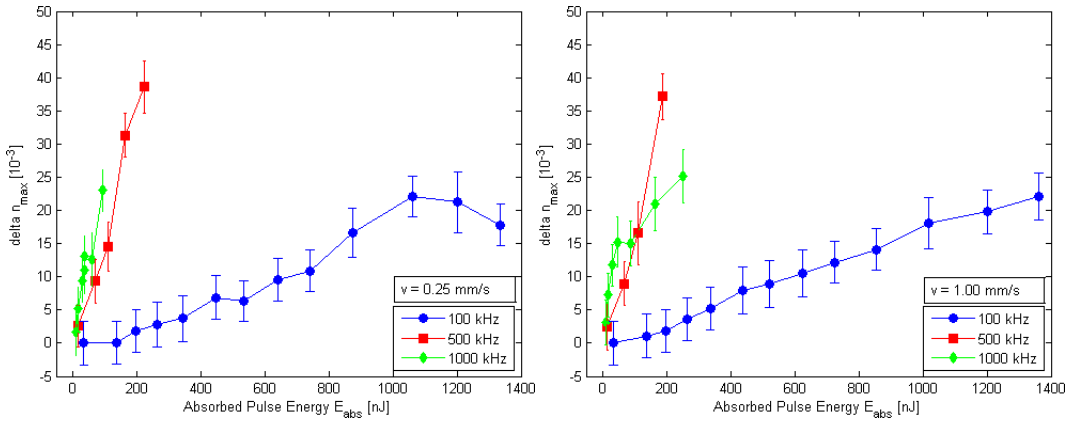

Figure 8 Maximum refractive index change Δn_{max} in Borofloat 33 for v =0.25mm/s (left) and v =1.00mm/s (right) at the investigated repetition rates

The maximum temperature change ΔT_{max} is observed for f_{rep} = 1000 kHz with ΔT_{max} ~ 5300 K. The maximum temperature change for f_{rep} = 100 kHz is calculated to ΔT_{max} ~ 3000 K. To achieve a temperature change of ΔT_{max} ~ 2000 K, a deposited energy of E_{tp} ~ 50 µJ/µm is required for v = 1.00 mm/s. The required deposited energy for v = 0.25 mm/s is E_{tp} ~ 225 µJ/µm.

The calculated maximum temperature change ΔT_{max} clearly depends on the velocity v and less on f_{rep}, thus E_{tp} is not the scaling physical quantity concerning the maximum temperature T_{max}. The calculated maximum temperatures are larger than the working temperature of the material T_{work} = 1250 °C. Therefore the observation of a heat affected zone can be explained. The calculation of the maximum temperature change ΔT_{max} is a first approximation of the real temperature during processing within the thermally affected material next to the central modification. On the one hand the temperature within the absorbing volume of the central modification is supposed to be higher than the calculated one. On the other hand the thermally affected material over and below the central modification leads to a higher measured OPD and thus to a higher refractive index and temperature. For more detailed investigations not only coaxial observation is needed, but also lateral measurements. These results can be combined like in a tomography in order to determine the spatial refractive index distribution and enable an abel inversion.

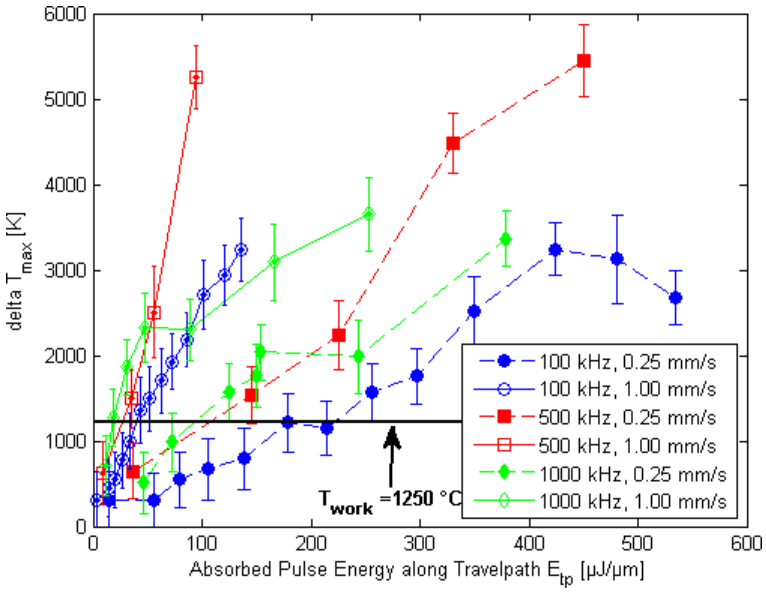

Figure 9 Calculated maximum temperature change ΔT_{max} in Borofloat 33 for different scanning velocities v and repetition rates f_{rep}

4. SUMMARY & OUTLOOK

Interference microscopy enables the measurement of the transient refractive index change in the material and thus the temperature estimation during material processing. A Mach-Zehnder interference microscope has been successfully setup and is operative for further time-averaging process investigations, together with a program for the automated analysis of interference images. Analysis during material processing of glass provides optical path difference (OPD) distributions for the different parameter settings to calculate upper and lower boundaries of the processing temperature. The processing temperature is estimated according to the observed morphology of the remanent modifications. The maximum calculated temperature change while processing the material is calculated to $\Delta T = 2000 - 5000$ K, whereas the calculation depends on the assumed coefficient dn/dT. This calculation is supported by the observation of a heat affected zone by light microscopy. Temperatures higher than the work temperature are necessary for the formation of a heat affected zone. Also these results are supported by calculations performed by Miyamoto. First proposed quantity *absorbed energy along travelpath* seems not to be the scaling physical quantity to describe the process.

Large repetition rates and scanning velocities of the focused laser radiation enable an absorptivity of up to 70% within the material. Further experiments with interference microscopy will investigate the temperature distribution at larger scanning velocities $v > 100$ mm/s and tomography should be performed in order to calculate an exact refractive index distribution and thus calculate the corresponding temperature field. The calculated temperature fields could verify simulations, e.g. those by Miyamoto [1].

REFERENCES

[1] K. Miura et al, “Photowritten optical waveguides in various glasses with ultrashort pulse laser”, Appl. Phys. Lett. 71 (23) (1997)

[2] Y. Bellouard et al, “Fabrication of high-aspect ratio , micro-fluidic channels and tunnels using fs-laser pulses and chemical etching”, Opt. Express 12, No.10 (2004)

[3] A. Horn, „Zeitaufgelöste Analyse der Wechselwirkung von ultrakurz gepulster Laserstrahlung mit Dielektrika“, Dissertation, Lehrstuhl für Lasertechnik, RWTH Aachen

[4] J. Song, “Self-trapped excitons in quartz and amorphous silica”, APS Meeting Abstracts, 31005 ff. (2000)

[5] A. Mermillod-Blondin et al, “Flipping the sign of refractive index change in ultrafast and temporally shaped laser-irradiated borosilicate crown optical glass at high repetition rates”, Physical Review B, 77: 104205 (2008)

[6] S. Eaton et al, “Heat accumulation effects in femtosecond laser-written waveguides with variable repetition rate”, OPTICS EXPRESS 4708 / Vol.13, No. 12 (2005)

[7] I. Miyamoto et al, “Fusion Welding of Glass Using Femtosecond Laser Pulses with High-repetition Rates”, JLMN-Journal of Laser Micro/Nanoengineering, Vol. 2, No. 1: 57-63 (2007)

[8] D. Leviton et al, “Temperature-dependent absolute refractive index measurements of synthetic fused silica”, Proc. of SPIE Vol. 6273, 62732K, (2006)

[9] J. Matsuoko et al, “Temperature dependence of refractive index of SiO2 glass”, Journal of Non-Crystalline Solids 135, 86-89 (1991)

[10] SCHOTT AG, „Borofloat 33 – Produktinformation“, http://www.schott.com/borofloat/german/ (2011)